

Dear Author,

Please, note that changes made to the HTML content will be added to the article before publication, but are not reflected in this PDF.

Note also that this file should not be used for submitting corrections.



Contents lists available at ScienceDirect

European Journal of Pharmaceutics and Biopharmaceutics

journal homepage: www.elsevier.com/locate/ejpb

Estimation of design space for an extrusion–spheronization process using response surface methodology and artificial neural network modelling

Tamás Sovány^{a,*}, Zsófia Tislér^a, Katalin Kristó^a, András Kelemen^b, Géza Regdon Jr.^a^a Department of Pharmaceutical Technology, University of Szeged, Eötvös u. 6, H-6720 Szeged, Hungary^b Department of Computer Sciences, University of Szeged, Boldogasszony sgt. 6, H-6725 Szeged, Hungary

ARTICLE INFO

Article history:

Received 31 August 2015

Revised 11 May 2016

Accepted in revised form 13 May 2016

Available online xxxxx

Keywords:

Extrusion–spheronization

Quality by Design

Response surface methodology

Artificial neural networks

ABSTRACT

The application of the Quality by Design principles is one of the key issues of the recent pharmaceutical developments. In the past decade a lot of knowledge was collected about the practical realization of the concept, but there are still a lot of unanswered questions.

The key requirement of the concept is the mathematical description of the effect of the critical factors and their interactions on the critical quality attributes (CQAs) of the product. The process design space (PDS) is usually determined by the use of design of experiment (DoE) based response surface methodologies (RSM), but inaccuracies in the applied polynomial models often resulted in the over/underestimation of the real trends and changes making the calculations uncertain, especially in the edge regions of the PDS. The completion of RSM with artificial neural network (ANN) based models is therefore a commonly used method to reduce the uncertainties. Nevertheless, since the different researches are focusing on the use of a given DoE, there is lack of comparative studies on different experimental layouts. Therefore, the aim of present study was to investigate the effect of the different DoE layouts (2 level full factorial, Central Composite, Box–Behnken, 3 level fractional and 3 level full factorial design) on the model predictability and to compare model sensitivities according to the organization of the experimental data set.

It was revealed that the size of the design space could differ more than 40% calculated with different polynomial models, which was associated with a considerable shift in its position when higher level layouts were applied. The shift was more considerable when the calculation was based on RSM. The model predictability was also better with ANN based models. Nevertheless, both modelling methods exhibit considerable sensitivity to the organization of the experimental data set, and the use of design layouts is recommended, where the extreme values factors are more represented.

© 2016 Elsevier B.V. All rights reserved.

1. Introduction

Biotechnologically produced active pharmaceutical ingredients (APIs), such as monoclonal antibodies, enzymes or other proteins and peptides have increasing importance in the pharmaceutical industry. A breakthrough is expected because of these APIs in the treatment of numerous severe conditions such as cancer, autoimmune or neurodegenerative diseases. Nevertheless, their production and processing is challenging because of their high sensitivity to the change of the environmental parameters, which may cause misfolding and loss of activity [1–3].

These APIs are mostly used in parenteral administration, but there is a great demand to change to oral formulations. Nevertheless, the low gastric pH, the presence of digestive enzymes and the poor absorption capacity of the highly hydrophilic macromolecules result in the poor bioavailability of such therapeutic agents [4].

There are many methods found in the literature dealt with the increase of the oral bioavailability of proteins. Enteric coatings [5], enzyme inhibitors [6,7], hydrogels [8], solid in oil formulations [9], liposomes [10] or other polymer nano- or microparticles [11–15] are used to protect the API from the gastrointestinal conditions. Liposomes, or functionalized microparticles may also increase the intestinal absorption. However, despite the numerous advantages, the difficult production method, the stability issues and the poor entrapment efficiency are considerable drawbacks of these formulations [10]. Furthermore, the appropriate administration of these delivery systems requires further formulation into different dosage

* Corresponding author.

E-mail address: t.sovany@pharm.u-szeged.hu (T. Sovány).

forms, which means extra stress on the protein containing systems. From an industrial aspect, the use of conventional dosage forms combined with absorption enhancers and mucoadhesive coatings to prolong the GI residence time in the site of absorption seems to be a more reliable solution [16,17]. The use of special absorption sites, such as buccal or sublingual mucosa is also a promising way to decrease the number of critical issues of oral protein administration [11].

As it was characterized in the previous paragraph, protein formulation has numerous critical issues, and the assurance of the appropriate bioavailability requires the application of complex delivery systems. Formulating proteins into multiparticulate dosage forms may decrease the risks from the damaged protective mechanisms (e.g. ruptured coating, insufficient release of enzyme inhibitors, etc.) and may provide better controllable drug release kinetics. Nevertheless, since granulation/pelletization is a complex and highly variable process [18], the use of Quality by Design (QbD) principles and appropriate modelling methods is essential to ensure the required quality of the product and protect the enzyme from the thermal and mechanical stresses induced by the production process [1–3,17,18].

One of the most critical issues of QbD methodology is the determination of the process design space (PDS) [19,20]. The PDS is a multivariate combination of the process parameters where the required values of the critical quality attributes (CQAs) of the product can be ensured. According to the relevant ICH guidelines [21–23], there is no need for process revalidation or applying change control protocols when the process parameters are changed within those ranges. The authorities require a complete mathematical description of the influence of critical process parameters (CPPs) on CQAs, and the clarification of the effect of factor interactions. The determination of factor interactions necessitates the use of design of experiment (DoE) based selection of experimental settings, instead of the formerly used changing one factor at a time in a sequential testing (COST or OFAT) based selection methods. As Eriksson [24] mentions in his book the COST based methods do not necessarily provide information on the optimum conditions and definitely no information on factor interactions. In contrast DoE, which varies all factors at the same time, according to a special algorithm provides different level information on both linear and nonlinear main factor effects and factor interactions, depending on the number of the applied experimental settings [24]. Nevertheless, the mathematical models describing the response surface are usually limited for linear or second order polynomials and have limited predictive force. There are numerous studies which investigated the possibilities to improve the reliability of the PDS and achieve better predictions of the product behaviour [25,26], with the combination of DoE with multivariate data analysis [27–30], data resampling [31,32], and advanced nonlinear modelling methods such as genetic algorithms or artificial neural networks (ANNs) [33–36]. ANNs are self-adaptive, iterative algorithms mimicking the learning mechanism of the human brain [37,38]. ANNs have numerous advantages over a simple DoE based statistical data analysis. ANNs may be associated with a wide range of functions (polynomial, exponential, logarithmic, power, etc.), and can handle large datasets and factors which are non-controllable due to economical and/or technical reasons and therefore cannot be implemented into the DoE. Furthermore, their structure is less hierarchical and more flexible in comparison with DoE, which helps the integration of data from routine production batches into the analysis.

Despite the numerous studies published on the combination of DoE with advanced nonlinear modelling techniques, there is a lack of information on how the applied DoE layout and the organization of the resulting experimental data set influence the reliability of the determined PDS. The reason for this phenomenon is that the relevant papers use a given experimental layout for the investigation

of the given problem, without involving additional data into the analysis.

In order to resolve this problem, the present work is focusing on the determination of the effect of the application of various DoE layouts on the reliability of the PDS determination. The work is based on our previous study [39] on the formulation of a solid multiparticulate system for lysozyme delivery. Lysozyme is a natural enzyme with antimicrobial, anti-inflammatory and immunomodulator activity. In the past years it has re-emerged as a topic for research since the number of antibiotic resistant bacteria tribes increased extensively. It can also be used in paediatrics as a comfortable and harmless treatment of GI infections [40] and inflammatory diseases.

2. Materials and methods

2.1. Materials

Crystalline egg-white lysozyme was purchased from Handary S. A. (Lysoch 40000, Handary S.A., Brussels, Belgium). Mannitol (Hun-garopharma, Budapest, Hungary) was used as a stabilizer and microcrystalline cellulose (Avicel PH 101, FMC Biopolymer, Philadelphia, USA) as a plastic carrier in the formulations.

2.2. Methods

10 g of lysozyme, 40 g of mannitol and 50 g of cellulose were homogenized in a Turbula mixer (Willy A. Bachofen Maschinenfabrik, Basel, Switzerland) for 10 min.

The homogenized powder mixture was wetted and kneaded in a ProCepT 4M8 high-shear granulator (ProCepT nv., Zelzate, Belgium) with 60 ml of purified water. CPPs (impeller and chopper speed, liquid addition rate, impeller torque and temperature) were recorded throughout the process.

The wet mass was extruded with a Caleva mini screw extruder (Caleva Process Solutions Ltd., Sturminster Newton, UK) and then spheronized with a Caleva MBS spheronizer (Caleva Process Solutions Ltd., Sturminster Newton, UK). The extruder was water-cooled with the application of a laboratory-developed cooling jacket, and the temperature was monitored with a laser thermometer every 30 s. The moisture content of the mass was checked continuously during extrusion and spheronization, with halogen moisture content analyser (Mettler Toledo Hungary Ltd., Budapest, Hungary) using 1 g of samples and 105 °C drying temperature. The extruded samples were stored in tightly-closing containers so as to avoid evaporation and decrease of the moisture content of the extruded mass before spheronization. The particles were spheronized at 2000 rpm friction plate speed for 15 min. The spheronized samples were dried for 24 h at room temperature.

The activity of pellets was determined via the degradation of *Micrococcus lysodeicticus* (VWR International, Budapest, Hungary). 25 mg of the lyophilized bacteria was suspended in 100 ml of pH 6.24 phosphate buffer. The basic absorbance of the suspension at 450 nm was approx. 0.7. 10 mg of lysozyme or 100 mg of pellets was dissolved in 25 ml of phosphate buffer, 2.5 ml of the suspension was measured into a 1 cm quartz cell, 0.1 ml of sample was added to the suspension and the absorbance was recorded every 5 s for 5 min. Since the error of activity determination when it was calculated from the absorbance change during a 1 min interval at the maximum linear rate was too high, the activity of the pellets was expressed as a percentage of the activity of the native lysozyme, based on the speed rates of the fitted exponential decay curves.

A Zeiss stereomicroscope (Carl Zeiss, Oberkochen, Germany) and Leica Quantimet 500 C image analysis software (Leica

Microsystems, Wetzlar, Germany) were used for the determination of the size and shape of the pellets. The length, width, perimeter, area and aspect ratio of the pellets were measured or calculated.

The hardness of the pellets was tested with a special hardness testing apparatus developed at the Department of Pharmaceutical Technology, University of Szeged. A vertical load is exerted on the pellets by a conical breaking item with 2 mm in diameter breaking surface. The force required for the deformation and breaking of pellets is detected by a 50 N load cell mounted to the bottom of the sample holder table, and recorded with 50 Hz sampling frequency during the whole deformation process. A general breaking curve and the discussion of the breaking process are presented in our previous paper [39].

The DoE and the statistical analysis of the results were performed with the application of Statistica for Windows v 12.0 (Statsoft Inc., Tulsa, OK, USA) software. The detailed description of the factor selection and justification of the determination of minimum and maximum settings may be found in our previous paper [39]. The advanced nonlinear modelling was performed with the help of a feed forward backpropagation algorithm using NNModel 32 v. 1.0.2.0 (Neural Fusion Shareware) software.

3. Results and discussion

One of the key issues of the QbD is the determination and verification of the PDS [19,20]. The present work was focused on the research of how the applied design layout influences the estimation and prediction accuracy of PDS. A 3³ full factorial DoE was performed with 2 randomized replications on the basis of the previous study [39]. The studied factors were impeller speed (*x*1) and liquid addition rate (*x*2) in the kneading phase and extrusion speed (*x*3). As CQAs, the enzymatic activity and the shape and hardness of the pellets were investigated. The detailed experimental settings and the corresponding results (mean and relative standard deviations (RSD)) are displayed in Table 1. The data were selected and analysed according to the requirements of different experimental layouts (2

Table 2

Results of the statistical analysis.

Design layout	Activity		Hardness ^a		Aspect ratio ^a	
	R ²	MS residual	R ²	MS residual	R ²	MS residual
2 level full	0.9886	84.27	0.7347	12.30	0.4325	0.0016
Central composite	0.7925	158.47	0.6164	11.57	0.3783	0.0014
3 level fractional	0.7892	103.68	0.5562	19.81	0.2846	0.0042
Box–Behnken	0.8111	146.44	0.5097	21.79	0.4703	0.0023
3 level full	0.8427	131.34	0.3211	25.49	0.3625	0.0019

^a The curvature check showed a significant presence of nonlinearity, and the best models are highlighted with boldfaced letters.

level full factorial, face centred central composite, Box–Behnken, 3 level fractional, 3 level full factorial).

The descriptive model was fitted to the results on the basis of linear regression using the least squares method. The fitting accuracy was evaluated with the goodness of fit (*R*²) and mean squared distance of data points from the fitted model (MS Residual) (Table 2). The significance of the factor coefficients (change of the CQA when a factor is raised from 0 to +1 level) was evaluated with two-way ANOVA test. The coefficients from the equations of the response surfaces are displayed in Table 3.

The results showed that the effect of some factors and factor interactions results in a significant nonlinearity in the behaviour of pellet hardness and aspect ratio. The applied test calculates the distance of the centre point from the linear model fitted to the corner points of the experimental settings to test the model adequacy. If the distance is insignificant, the use of the linear model is appropriate, if not, nonlinear models should be applied [24]. In the case of enzyme activity, the result of the nonlinearity test was statistically insignificant, probably due to the fact that high standard deviation of the activity results in the centre point of experiments. Nevertheless, the considerable high value of the

Table 1

Settings and results of the DoE.

Impeller speed (<i>x</i> 1) (rpm)	Liquid addition rate (<i>x</i> 2) (ml/min)	Extruder speed (<i>x</i> 3) (rpm)	Activity (%)		Hardness (N)		Aspect ratio	
			Mean	RSD (%)	Mean	RSD (%)	Mean	RSD (%)
500	5	70	88.19	13.25	18.99	13.70	1.20	7.20
500	5	95	85.48	8.81	20.35	64.31	1.23	4.84
500	5	120	70.08	12.47	25.99	14.08	1.17	1.24
500	7.5	70	74.60	6.50	15.14	13.60	1.21	2.46
500	7.5	95	87.19	5.86	17.37	13.13	1.19	0.60
500	7.5	120	47.72	41.59	17.45	7.88	1.20	2.73
500	10	70	40.00	13.79	14.55	30.15	1.26	4.48
500	10	95	88.49	6.36	19.84	19.78	1.27	10.24
500	10	120	49.90	21.31	9.05	11.73	1.21	0.56
1000	5	70	72.15	0.92	22.42	10.43	1.18	2.75
1000	5	95	77.71	5.11	14.49	6.91	1.22	2.57
1000	5	120	85.23	4.61	8.60	26.90	1.26	3.45
1000	7.5	70	42.86	9.11	20.36	16.26	1.18	1.03
1000	7.5	95	49.73	30.16	21.03	13.19	1.15	1.72
1000	7.5	120	48.01	30.15	20.43	7.12	1.19	2.22
1000	10	70	80.52	6.01	9.15	86.40	1.19	0.49
1000	10	95	80.09	6.90	20.73	2.43	1.19	4.44
1000	10	120	81.60	3.52	17.16	25.47	1.21	1.96
1500	5	70	55.48	21.44	11.14	43.00	1.20	1.12
1500	5	95	90.36	4.44	17.04	25.64	1.22	7.62
1500	5	120	65.58	21.87	14.10	11.04	1.20	2.75
1500	7.5	70	84.70	7.66	18.53	18.57	1.22	1.04
1500	7.5	95	70.69	20.85	18.22	12.50	1.26	1.33
1500	7.5	120	46.91	17.07	14.20	21.27	1.26	2.13
1500	10	70	38.85	9.99	18.13	21.78	1.18	1.38
1500	10	95	85.37	6.19	17.48	3.46	1.24	1.49
1500	10	120	63.72	11.00	13.96	39.22	1.23	3.32

Table 3
Coefficients of response surface equations.

Factor	Design type	b_0	b_1	b_{11}	b_2	b_{22}	b_3	b_{33}	b_{12}	b_{122}	b_{112}	b_{1122}	b_{13}	b_{133}	b_{113}	b_{1133}	b_{23}	b_{233}	b_{223}	b_{2233}	
Activity	2 ³	58.98	3.07		10.86		3.34		6.23				5.40				5.35				
	CC	62.10	-4.10	10.66	-8.44	10.61	3.19	22.85	6.23				5.39				5.34				
	3 ³⁻¹	75.41	2.39	2.69	5.17	11.01	9.45	5.55	12.2	9.95											
	BB	76.93	1.38	-5.32	0.34	13.52	6.31	1.55	2.00	0.94	0.83			2.73	9.85		3.00				
3 ³	68.56	1.66	0.07	-4.54	5.39	1.03	8.17	3.49	0.34	4.29	-8.22		2.68	0.59	3.19	5.83	2.56	3.45	6.66	1.73	
Hardness	2 ³	15.74	1.82		1.41		0.03		3.53				2.45				0.34				
	CC	20.48	1.37	2.41	0.50	2.59	0.03	0.19	3.53				2.45				0.34				
	3 ³⁻¹	15.62	0.44	2.02	0.98	2.58	1.25	3.50	3.56	0.25											
	BB	16.45	0.93	0.09	0.41	1.09	0.82	2.26	0.24	0.73	0.58			1.66	0.47		5.45				
3 ³	16.88	0.88	0.20	0.72	0.89	-0.41	1.22	2.43	0.78	0.73	1.27	0.78	0.06	0.41	0.01	0.18	1.32	0.07	0.47		
Aspect ratio	2 ³	1.21	0.014		0.005		0.003		0.011				0.002				0.02				
	CC	1.18	0.019	0.029	0.007	0.008	0.000	0.006	0.012				0.002				0.016				
	3 ³⁻¹	1.22	0.001	0.012	0.002	0.019	0.034	0.018	0.035	0.033											
	BB	1.22	0.0003	0.026	0.007	-0.02	0.012	0.009	0.003	0.013	0.011			0.011	0.009		0.01				
3 ³	1.22	0.003	0.012	0.006	0.004	0.006	0.005	0.009	0.015	0.012	0.009	0.015	0.002	0.009	0.010	0.004	0.001	0.0002	0.008		

2³: 2 level full factorial design, CC: Face-centred central composite design, 3³⁻¹: 3 level fractional design, BB: Box–Behnken design, 3³: 3 level full factorial design; significant factors and factor interactions are shown with boldface type.

258 curvature coefficient indicated the presence of nonlinearity. It was
 259 confirmed that a considerable drawback of the use of the DoE
 260 based RSM is that although the use of second order polynomial
 261 equations may add extra information and enhance the process of
 262 understanding whether a nonlinear relationship exists between
 263 critical process parameters (CPPs) and CQAs, it is notable that the
 264 increment of the number of experiments did not necessarily result
 265 in a better fitting model. Furthermore, as it is well visible, the
 266 weight of the single coefficients decreased with the increment of
 267 the number of experimental settings (Table 3). In this particular
 268 case, it was a general tendency that the significance of the coeffi-
 269 cients shifted from the linear to the nonlinear elements and from
 270 the single nonlinear effects to the nonlinear interactions, which
 271 indicated the complexity of effect of CPPs to CQAs. The presence
 272 of significant second order factor interactions made the interpreta-
 273 tion of the models and the determination of the effect of the single

274 factor changes extremely difficult, since in these complex systems
 275 the effect of a minor change had a great effect on the behaviour of
 276 the whole system.

277 The evaluation of the prediction performances of the different
 278 models was based on the testing of the correlation of observed
 279 and predicted values. Fig. 1 displays the prediction results for
 280 enzyme activity according to the different DoE layouts and evalua-
 281 tion methods. It is well visible that the use of ANN based evalua-
 282 tion resulted in better correlation of the measured and predicted
 283 values than RSM. It is notable that linear estimation provided poor
 284 predictability despite the nonlinear effects being estimated as
 285 insignificant in the RSM. The best predictions were given by Central
 286 Composite design where the weight of nonlinear parameters
 287 in the response surface equation is smaller. This can be due to
 288 the fact that the parabolic function is not suitable for the modelling
 289 of a complex surface since it cannot detect the slight changes of

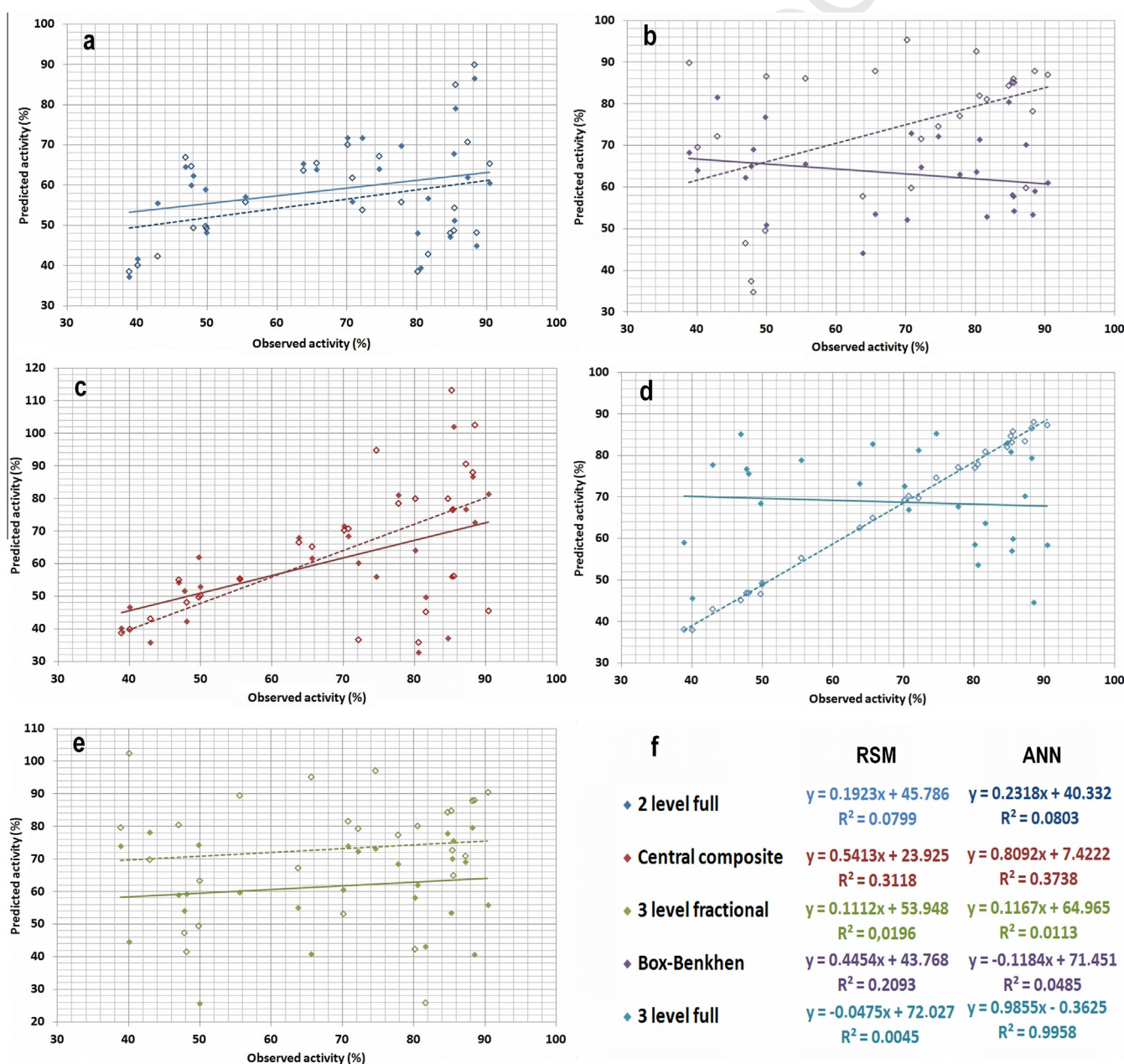


Fig. 1. Observed vs. predicted data plots (full line: RSM, dashed line: ANN) on the modelling of enzyme activity. (a) 2 level full factorial design, (b) central composite design, (c) 3 level fractional, (d) Box-Behnken design, (e) 3 level full factorial design, (f) equations and R^2 values of the linear regression on the observed vs. predicted data.

parameters and considerably under/overestimates the real values in those regions where the response function changes its sense. This effect was more considerable if the combinations where at least 2 factors are on minimum or maximum levels were missing from the experimental data set used for model building (3 level fractional, Box–Behnken). The differences in model predictability were similar also for hardness and aspect ratio, see the electronic Supplementary material.

To unfold these problems and to compare the predictive force of a higher level nonlinear modelling technique with the conventional DoE based RSM, an ANN based model was developed on the basis of a combination of genetic algorithm and manual screening process (Fig. 2). The data pairs from the repeated DoE were used to train and test the ANN. Therefore, the number of data points was different according to the number of the experimental settings used in the different DoE layouts. 80% of the randomly selected data points were used for training while the remaining 20% was retained for the testing of model predictability according to a repeated leave-p-out cross-validation method. A genetic algorithm was used for the determination of the optimal number of hidden neurons. The algorithm analysed the progress of training statistically via the improvement of the error tolerance, and increased the number of hidden neurons in an iterative way. A new hidden neuron was added to the system if the improvement of the observed vs. predicted R^2 statistics decreased below 0.005 in a 100 epoch window. The momentum of the learning was 0.8 and 0.5 was selected as threshold value. The modification of these values did not result in any significant improvement. The learning rates were kept as defaults 0.75 and 1.5 of the input to hidden and hidden to output layer, respectively. Nevertheless, a 0.75 value was selected to decrease the initial learning rates when an extra neuron was added to the system. The maximum number of hidden neurons was set to 20, and the maximum number of learning cycles was 1 million. Three different stopping criteria were applied. The learning procedure would be stopped if all the predicted values were within the $\pm 5\%$ tolerance band of the accepted total error or the sum-of-square error function decreased below 0.001, or the

overall R^2 value of the observed vs. predicted correlations was over 0.95. Nevertheless, none of the stopping criteria was reached within the applied maximum of the learning cycles. Since the improvement of the prediction accuracy followed a saturation curve with the increment of the number of hidden neurons and learning cycles, a certain improvement required too long time after a given level. Therefore, the number of neurons and the learning cycles were selected as optimal where the curve started to turn into steady state.

Since the applied genetic algorithm decreased the speed of convergence and required longer learning time, the experiments were repeated with fixing the optimal neuron number. The other parameters were the same as the ones used in the genetic algorithm. Under these conditions the convergence of the system was much faster; however, the chaotic working and oscillation of the prediction performance were increased with the default learning rates. To unfold these problems, a manual screening was performed to find the optimal value of the learning rates, according to a 3^2 level full factorial design. The default learning rates were selected as +1 level, and the values were decreased in a logarithmic scale for 0 and -1 levels. The results showed that the decrease of the learning rates unfolded the problem of the oscillating predictions and provided a much smoother learning procedure with better overall prediction performance. Nevertheless, since the use of the learning rates in -1 level doubled the required learning time, and the improvement in predictive force was decreased between 0 and -1 compared to the decrease from +1 to 0, no further improvement was expected as a result of a further decrease.

The optimal neuron numbers were 7, 5, 8, 9 and 14 for the 2 level full factorial, 3 level fractional, Box–Behnken, Central Composite and 3 level full factorial design, respectively. According to the experimental results, the approximately optimal training length could be calculated using the following equation:

$$\text{No. of learning cycles} = 90,000 * \text{No. experimental data sets} / \text{No. of neurons}$$

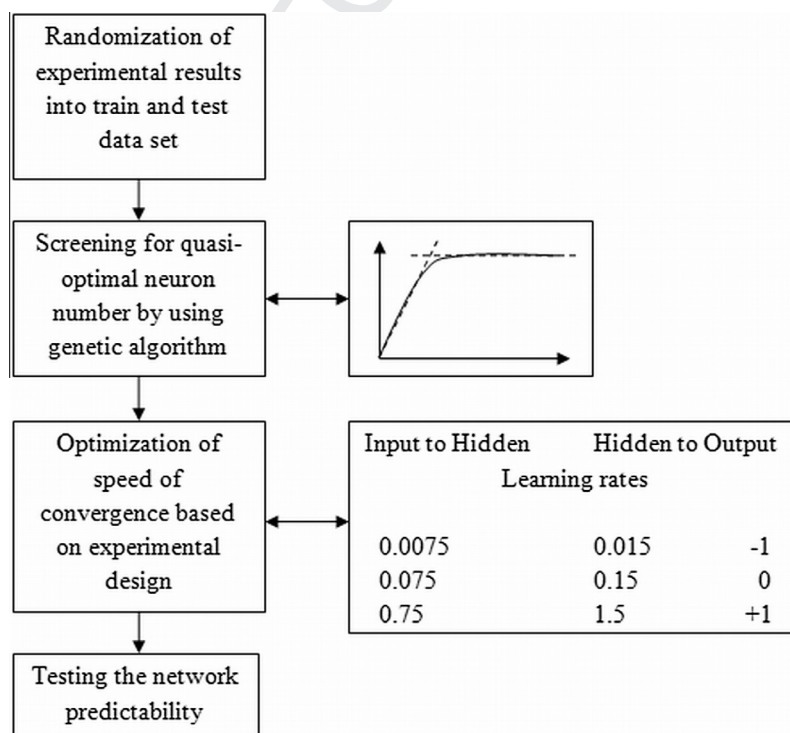


Fig. 2. Flow chart of the ANN optimization process.

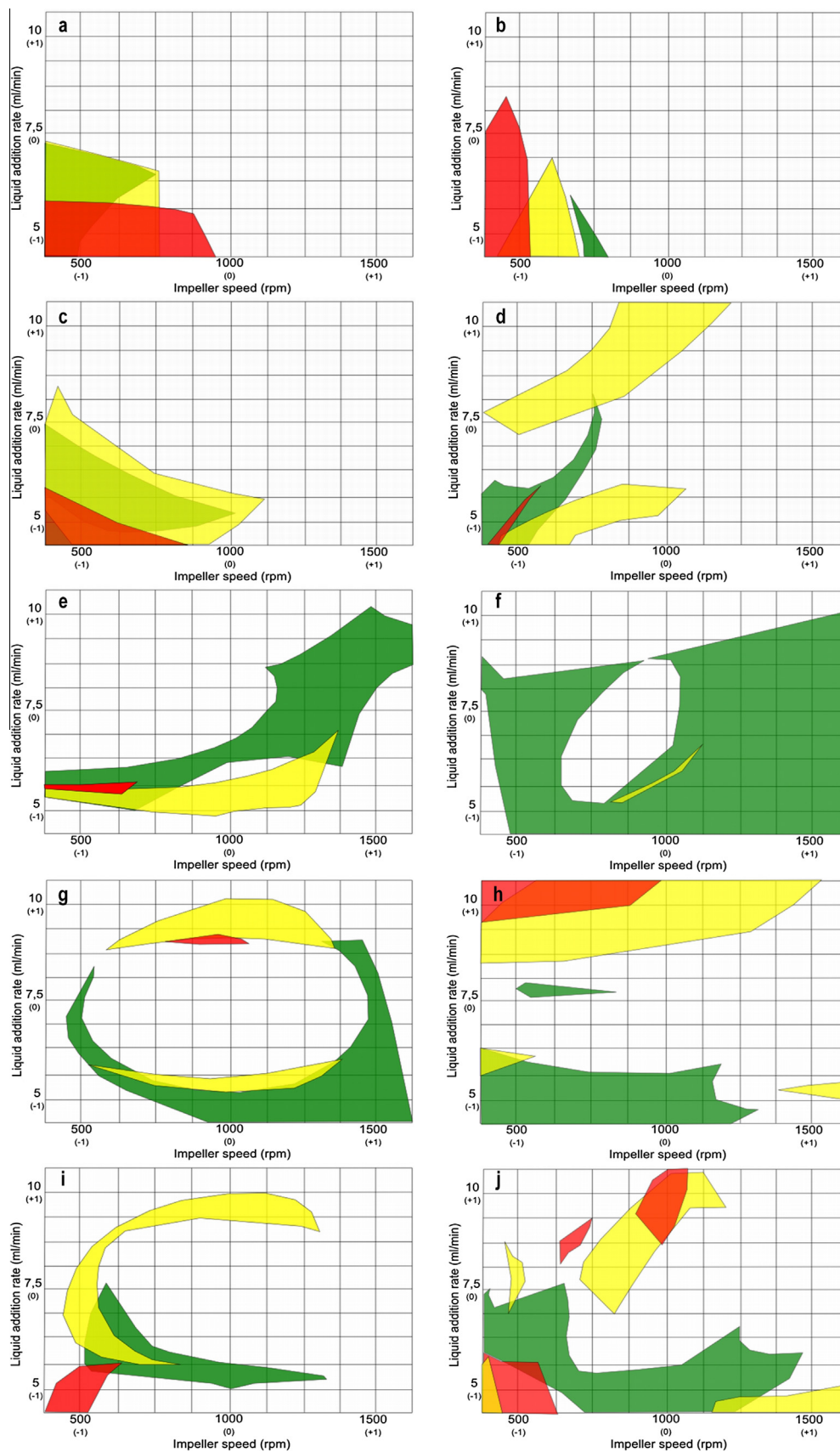


Fig. 3. Design spaces calculated from the results of different design of experiment layouts and modelling techniques. (a) 2 level full factorial RSM, (b) 2 level full factorial ANN, (c) central composite RSM, (d) central composite ANN, (e) 3 level fractional RSM, (f) 3 level fractional ANN, (g) Box–Behnken design RSM, (h) Box–Behnken design ANN, (i) 3 level full factorial RSM, (j) 3 level full factorial ANN, (extrusion speed is 70 rpm (green area), 95 rpm (yellow area) and 120 rpm (red area)). (For interpretation of the references to colour in this figure legend, the reader is referred to the web version of this article.)

The convergence in linear estimation required shorter time compared to the different level nonlinear estimations. For the further improvement of the learning efficacy, the integration of the backpropagation algorithm with a conjugate gradient algorithm was also tested. However, it did not result in any considerable improvement.

The prediction capability of the different models was tested based on leave-p-out cross validating in multiple rounds, using 20% of the existing data as test set in the training phase. The final testing of the predictive force and model building capability of the ANN and the comparison with the same values obtained from DoE was based on the testing of the correlation of the observed and predicted data of all applied data points.

The results confirmed the preliminary expectations that the ANN provides better predictions. The observed vs. predicted correlation was better with one order of magnitude in most of the tested cases. Nevertheless, the ANN based models exhibited similar sensitivity to the lack of extremes in the data set as the RSM. However, the effect of the applied number of data sets was in contradiction with the RSM results, since the prediction efficacy considerably improved with the increment of the number of data used for training.

By comparing the RSM and ANN models it can be seen that there were extreme differences in the PDSs calculated according to the different DoE layouts and to the evaluation method (Fig. 3). The nonlinear models were usually strongly narrowing the PDS and the above mentioned fitting issues and underestimations may lead to the misinterpretation of the results due to the cumulative effect of the estimation errors in the calculation of the different CQAs. The effect of model based estimation errors may be decreased by the matching of PDSs calculated with RSM and ANN and applying the common region as PDS. The application of ANN models also has the advantage that the results of the routine production can be used for the improvement of the model accuracy since it was found that the increasing number of data points in the training data set continuously improves the predictive force of the model.

4. Conclusions

Determination of the PDS is still a key issue of the Quality by Design principles. The reliability of the calculated PDS highly depends on the applied experimental data set. In the present study the effect of the number and organization of the experimental data points was tested on the result of an optimization process based on RSM or ANN based modelling. The results revealed that the increment of the number of data points does not necessarily improve the predictive force of the model. This can be due to the use of second order polynomials to describe the response surface, which may lead to over/underestimation of the real trends. It was confirmed that the predictive force of ANN based models is superior over RSM and provides better robustness for PDS determination. Furthermore, the ANN predictability may be significantly improved with the increment of training data points.

Nevertheless, it is notable that both RSM and ANN exhibited considerable sensitivity to the organization of the experimental data set, especially if it contained a similar number of data points. In comparison with the various experimental layouts it can be stated that those models in which a higher number of extreme factors are involved give considerably better predictions.

The uncertainties in the estimation of the acceptance regions of CQAs due to the model fitting issues will be present in a cumulative way in the estimation of PDS. Based on our findings, the use of central composite design is highly recommended to build the mathematical model of PDS. Nevertheless, the matching of RSM with ANN based results is also highly recommended to decrease

the uncertainties and the risks of data misinterpretation. The retrain of ANNs with data of commercial production may improve PDS reliability during the lifecycle of the product, but the enlargement of the training data set may require the modification of the network texture.

Acknowledgements

This research was supported by the European Union and the State of Hungary, co-financed by the European Social Fund in the framework of TÁMOP 4.2.4. A/2-11-1-2012-0001 'National Excellence Program'.

Appendix A. Supplementary material

Supplementary data associated with this article can be found, in the online version, at <http://dx.doi.org/10.1016/j.ejpb.2016.05.009>.

References

- [1] J. Chin, K.A.F. Mahmud, S.E. Kim, K. Park, Y. Byun, Insight of current technologies for oral delivery of proteins and peptides, *Drug Discov. Today* 9 (2012) 105–112.
- [2] J. Renukuntla, A.D. Vadlapudi, A. Patel, S.H.S. Boddu, A.K. Mitra, Approaches for enhancing oral bioavailability of peptides and proteins, *Int. J. Pharm.* 447 (2013) 75–93.
- [3] A. Muheem, F. Shakeel, M.A. Jahangir, M. Anwar, N. Mallick, G.K. Jain, M.H. Warsi, F.J. Ahmad, A review on the strategies for oral delivery of proteins and peptides and their clinical perspectives, *Saudi Pharm. J.* (2014), <http://dx.doi.org/10.1016/j.jsps.2014.06.004>.
- [4] B.F. Choonara, Y.E. Choonara, P. Kumar, D. Bijukumar, L.C. du Troit, V. Pillay, A review of advanced drug delivery technologies facilitating the protection and absorption of protein and peptide molecules, *Biotechnol. Adv.* 32 (2014) 1269–1282.
- [5] X. Zhang, W. Wu, Ligand-mediated active targeting for enhanced oral absorption, *Drug Discov. Today* 19 (2014) 898–904.
- [6] A. Maroni, L. Zema, M.D. Del Curto, A. Foppoli, A. Gazzaniga, Oral colon delivery of insulin with the aid of functional adjuvants, *Adv. Drug Deliv. Rev.* 64 (2012) 540–556.
- [7] E.J.B. Nielsen, S. Yoshida, N. Kamei, R. Iwamae, E.-S. Kafagy, J. Olsen, U.L. Rahbek, B.L. Pedersen, K. Takayama, M. Takeda-Morishita, In vivo proof of concept of oral insulin delivery based on a co-administration strategy with the cell-penetrating peptide penetratin, *J. Control. Release* 189 (2014) 19–24.
- [8] M.C. Koetting, N.A. Peppas, PH-Responsive poly(itaconic acid-co-N-vinylpyrrolidone) hydrogels with reduced ionic strength loading solutions offer improved oral delivery potential for high isoelectric point-exhibiting therapeutic proteins, *Int. J. Pharm.* 471 (2014) 83–91.
- [9] E. Toorisaka, K. Watanabe, H. Ono, M. Hirata, N. Kamiya, M. Goto, Intestinal patches with an immobilized solid-in-oil formulation for oral protein delivery, *Acta Biomater.* 8 (2012) 653–658.
- [10] J. Kowapardit, A. Apirakarmwong, T. Ngawhirunpat, T. Rojanarata, W. Sajomsang, P. Opanasopit, Methylated N-(4-N,N-dimethylaminobenzyl) chitosan coated liposomes for oral protein drug delivery, *Eur. J. Pharm. Sci.* 47 (2014) 359–366.
- [11] P.C. Christophersen, L. Zhang, M. Yang, H.M. Nielsen, A. Müllertz, H. Mu, Solid lipid particles for oral delivery of peptide and protein drugs I – elucidating the release mechanism of lysozyme during lipolysis, *Eur. J. Pharm. Biopharm.* 85 (2013) 473–480.
- [12] G. Ma, Microencapsulation of protein drugs for drug delivery: strategy, preparation, and applications, *J. Control. Release* 193 (2014) 324–340.
- [13] J.O. Morales, S. Huang, R.O. Williams III, J.T. McConville, Films loaded with insulin-coated nanoparticles (ICNP) as potential platforms for peptide buccal delivery, *Colloids Surf. B* 122 (2014) 38–45.
- [14] H.-P. Lim, B.-T. Tey, E.-S. Chan, Particle designs for the stabilization and controlled-delivery of protein drugs by biopolymers: a case study on insulin, *J. Control. Release* 186 (2014) 11–21.
- [15] C. He, L. Yin, C. Tang, C. Yin, Size-dependent absorption mechanism of polymeric nanoparticles for oral delivery of protein drugs, *Biomaterials* 33 (2012) 8569–8578.
- [16] V.F. Patel, F. Liu, M.B. Brown, Advances in oral transmucosal delivery, *J. Control. Release* 153 (2011) 106–116.
- [17] V.K. Pawar, J.G. Meher, Y. Singh, M. Chaurasia, B.S. Reddy, M.K. Chaurasia, Targeting of gastrointestinal tract for amended delivery of protein/peptide therapeutics: strategies and industrial perspectives, *J. Control. Release* 196 (2014) 168–183.
- [18] R.P.J. Sochon, S. Zomer, J.J. Cartwright, M.J. Hounslow, A.D. Salman, The variability of pharmaceutical granulation, *Chem. Eng. J.* 164 (2010) 285–291.
- [19] R.A. Lionberger, S.L. Lee, L.M. Lee, A. Raw, L.X. Yu, Quality by design: concepts for ANDAs, *AAPS J.* 10 (2008) 268–276.

- 499 [20] L.X. Yu, Pharmaceutical quality by design: product and process development, understanding, and control, *Pharm. Res.* 25 (2008) 781–791. 532
- 500 [21] ICH Topic Q8(R2), Guidance for Industry: Pharmaceutical Development 533
- 501 <[http://www.ich.org/fileadmin/PublicWebSite/ICHProducts/Guidelines/](http://www.ich.org/fileadmin/PublicWebSite/ICHProducts/Guidelines/Quality/Q8R1/Step4/Q8R2Guideline.pdf) 534
- 502 <[http://www.ich.org/fileadmin/PublicWebSite/ICHProducts/Guidelines/Quality/Q9/Step4/](http://www.ich.org/fileadmin/PublicWebSite/ICHProducts/Guidelines/Quality/Q9/Step4/Q9Guideline.pdf) 535
- 503 <[http://www.ich.org/fileadmin/PublicWebSite/ICHProducts/Guidelines/Quality/Q10/](http://www.ich.org/fileadmin/PublicWebSite/ICHProducts/Guidelines/Quality/Q10/Step4/Q10Guideline.pdf) 536
- 504 <[http://www.ich.org/fileadmin/PublicWebSite/ICHProducts/Guidelines/Quality/Q10/](http://www.ich.org/fileadmin/PublicWebSite/ICHProducts/Guidelines/Quality/Q10/Step4/Q10Guideline.pdf) 537
- 505 <[http://www.ich.org/fileadmin/PublicWebSite/ICHProducts/Guidelines/Quality/Q10/](http://www.ich.org/fileadmin/PublicWebSite/ICHProducts/Guidelines/Quality/Q10/Step4/Q10Guideline.pdf) 538
- 506 <[http://www.ich.org/fileadmin/PublicWebSite/ICHProducts/Guidelines/Quality/Q10/](http://www.ich.org/fileadmin/PublicWebSite/ICHProducts/Guidelines/Quality/Q10/Step4/Q10Guideline.pdf) 539
- 507 <[http://www.ich.org/fileadmin/PublicWebSite/ICHProducts/Guidelines/Quality/Q10/](http://www.ich.org/fileadmin/PublicWebSite/ICHProducts/Guidelines/Quality/Q10/Step4/Q10Guideline.pdf) 540
- 508 <[http://www.ich.org/fileadmin/PublicWebSite/ICHProducts/Guidelines/Quality/Q10/](http://www.ich.org/fileadmin/PublicWebSite/ICHProducts/Guidelines/Quality/Q10/Step4/Q10Guideline.pdf) 541
- 509 <[http://www.ich.org/fileadmin/PublicWebSite/ICHProducts/Guidelines/Quality/Q10/](http://www.ich.org/fileadmin/PublicWebSite/ICHProducts/Guidelines/Quality/Q10/Step4/Q10Guideline.pdf) 542
- 510 L. Eriksson, Design of Experiments: Principles and Applications, MKS Umetrics 543
- 511 AB, Malmö, Sweden, 2008. 544
- 512 [25] K.V. Gernaey, A.E. Cervera-Padrell, J.M. Woodley, A perspective on PSE in 545
- 513 pharmaceutical process development and innovation, *Comput. Chem. Eng.* 42 546
- 514 (2012) 15–29. 547
- 515 [26] N. Mennini, S. Furlanetto, M. Cirri, P. Mura, Quality by design approach for 548
- 516 developing chitosan–Ca–alginate microspheres for colon delivery of celecoxib- 549
- 517 hydroxypropyl- β -cyclodextrin–PVP complex, *Eur. J. Pharm. Biopharm.* 80 550
- 518 (2012) 67–75. 551
- 519 [27] H. Wu, M. Tawakkul, M. White, M.A. Khan, Quality-by-Design (QbD): an 552
- 520 integrated multivariate approach for the component quantification in powder 553
- 521 blends, *Int. J. Pharm.* 372 (2009) 39–48. 554
- 522 [28] J. Huang, G. Kaul, C. Cai, R. Chatlapalli, P. Hernandez-Abad, K. Ghosh, A. Nagi, 555
- 523 Quality by design case study: an integrated multivariate approach to drug 556
- 524 product and process development, *Int. J. Pharm.* 382 (2009) 23–32. 557
- 525 [29] H. Wu, M. White, M.A. Khan, Quality-by-Design (QbD): an integrated process 558
- 526 analytical technology (PAT) approach for a dynamic pharmaceutical co- 559
- 527 precipitation process characterization and process design space development, 560
- 528 *Int. J. Pharm.* 405 (2011) 63–78. 561
- 529 [30] V. Lourenço, D. Lochmann, G. Reich, J.C. Menezes, T. Herdling, J. Schewitz, A 562
- 530 quality by design study applied to an industrial pharmaceutical fluid bed 563
- 531 granulation, *Eur. J. Pharm. Biopharm.* 81 (2012) 438–447. 564
- 532 [31] Y. Onuki, K. Ohyama, C. Kaseda, H. Arai, T. Suzuki, K. Takayama, Evaluation of 533
- 534 the reliability of nonlinear optimal solutions in pharmaceuticals using a 534
- 535 bootstrap resampling technique in combination with Kohonen's self- 535
- 536 organizing maps, *J. Pharm. Sci. – US* 97 (2008) 331–339. 536
- 537 [32] Y. Hayashi, S. Kikuchi, Y. Onuki, K. Takayama, Reliability evaluation of 537
- 538 nonlinear design space in pharmaceutical product development, *J. Pharm. 538*
- 539 *Sci. – US* 101 (2012) 333–341. 539
- 540 [33] J. Djuris, D. Medarevic, M. Kristic, Z. Djuric, S. Ibric, Application of quality by 540
- 541 design concepts in the development of fluidized bed granulation and tableting 541
- 542 processes, *J. Pharm. Sci. – US* 102 (2013) 1869–1882. 542
- 543 [34] H.I. Labouta, L.K. El-Khordagui, A.M. Molokhia, G.M. Ghaly, Multivariate 543
- 544 modeling of encapsulation and release of an ionizable drug from polymer 544
- 545 microspheres, *J. Pharm. Sci. – US* 98 (2009) 4603–4615. 545
- 546 [35] V. Pillay, M.P. Danckwerts, Textural profiling and statistical optimization of 546
- 547 crosslinked calcium–alginate–pectinate–cellulose acetophthalate gelisphere 547
- 548 matrices, *J. Pharm. Sci. – US* 91 (2002) 2559–2570. 548
- 549 [36] T.B. Patel, L.D. Patel, T.R. Patel, B.N. Suhagia, Artificial neural networks as tool 549
- 550 for quality by design in formulation of solid dispersion of fenofibrate, *Bull. 550*
- 551 *Pharm. Res.* 5 (2015) 20–27. 551
- 552 [37] P.J. Braspenning, F. Thuijsman, A.J.M.M. Weijters, Artificial Neural Networks: 552
- 553 An Introduction to ANN Theory and Practice, Springer-Verlag GmbH, Berlin, 553
- 554 Germany, 1995. 554
- 555 [38] H. Tang, K.C. Tan, Z. Yi, Neural Networks: Computational Models and 555
- 556 Applications, Springer-Verlag GmbH, Berlin, Germany, 2007. 556
- 557 [39] T. Sovány, K. Csordás, A. Kelemen, G. Regdon Jr., K. Pintye-Hódi, Development 557
- 558 of pellets for oral lysozyme delivery by using a quality by design approach, 558
- 559 *Chem. Eng. Res. Des.* 106 (2016) 92–100. 559
- 560 [40] C.A. Rubio, The natural antimicrobial enzyme lysozyme is up-regulated in 560
- 561 gastrointestinal inflammatory conditions, *Pathogens* 3 (2014) 73–92. 561